

## Droplet-cluster transition in sheared polyamide 6–poly(styrene-ethylene-butadiene-styrene)–polypropylene ternary blends

Yutian Zhu,<sup>1</sup> Xiaodong Yang,<sup>2</sup> Jinghua Yin,<sup>1</sup> and Wei Jiang<sup>1,\*</sup>

<sup>1</sup>*State Key Laboratory of Polymer Physics and Chemistry, Changchun Institute of Applied Chemistry, Chinese Academy of Sciences, Changchun 130022, People's Republic of China*

<sup>2</sup>*Jilin Teachers Institute of Engineering and Technology, Changchun 130052, People's Republic of China*

(Received 25 April 2010; published 30 September 2010)

We have used a Linkam CSS 450 stage equipped with an optical microscope to study online the evolution of the morphology and structure of polyamide 6 (PA6)–poly(styrene-ethylene-butadiene-styrene) (SEBS)–polypropylene (PP) ternary blends under shear flow. At a high shear rate ( $60 \text{ s}^{-1}$ ), large drops of PA6 and SEBS broke up to form small randomly distributed PA6 droplets covered by SEBS in the PP matrix. These droplets aggregated into a well-ordered structure, i.e., parallel clusters, after decreasing the shear rate abruptly to within the range of  $1.5\text{--}3.5 \text{ s}^{-1}$ . Interestingly, these parallel clusters were aligned perpendicular to the direction of shear flow. An important feature of these parallel clusters is that they can be maintained for a long period of time (several tens of minutes) at the given shear rate or after cessation of flow; this feature allows us to freeze the structure by decreasing the temperature.

DOI: [10.1103/PhysRevE.82.031807](https://doi.org/10.1103/PhysRevE.82.031807)

PACS number(s): 61.25.hk, 83.50.Ax, 83.80.Tc

### I. INTRODUCTION

The properties of a polymer blend depend strongly on its morphology and structure. Shearing forces are among the most important factors that determine the formation of a certain morphology and structure during the processing of a given polymer blend. In general, the breakup [1,2] and coalescence [3,4] of dispersed droplets are two opposing trends that occur to a melting blend under a shear flow. Taylor provided a detailed analysis of this process for Newtonian fluids [1,2] and demonstrated that the capillary number could be determined using the following equation:

$$Ca = \eta_m \dot{\gamma} R / \sigma, \quad (1)$$

where  $\eta_m$  is the matrix phase viscosity,  $\dot{\gamma}$  is the applied shear rate,  $R$  is the droplet radius, and  $\sigma$  is the interfacial tension between the two phases. Once the value of  $Ca$  exceeds a critical value (0.5), breakup will occur under a steady shear until the system reaches a stable steady-state droplet diameter  $D_s$ , which is defined by the equation

$$D_s = \frac{2\nu Ca_{crit}}{\eta_m \dot{\gamma}} \approx \frac{\sigma}{\eta_m \dot{\gamma}}. \quad (2)$$

In contrast, coalescence is possible when the droplet size is smaller than the steady-state droplet size provided in Eq. (2). A distribution of droplet sizes is created during the break-up process [5–7]. As a result, coalescence of the small droplets may occur during a steady shear. Besides the breakup and coalescence, droplet deformation under an applied shear field and shape recovery during the relaxation are commonly encountered and extensively investigated for the immiscible polymer blends [8,9]. In addition, some groups also used the artificial capsule, i.e., a capsule consists of a

liquid drop surrounded by a deformable interface, instead of droplet to study the flow-induced deformation [10–14].

The formation of fluid-flow-induced patterns has been investigated widely. For instance, stringlike structures in flowed blends have been studied intensely for many years [15–21]. Mietus *et al.* [22] observed the formation of toroidal rings and water sheaths in the Couette flow of two immiscible liquids between concentric cylinders. In addition, the droplet vorticity alignment in sheared polymeric emulsions has been studied extensively over a broad range of physical systems [23–25]. In recent years, a number of novel ordered patterns—including anisotropic chainlike structures [26–32], anisotropic cluster structures [30], and hexagonal arrays [32–35]—have been observed to form from colloidal particles or droplets. Furthermore, Lin-Gibson *et al.* [36] reported that elastic instability was associated with flow-induced clustering in semidilute non-Brownian colloidal nanotubes. Recently, the process of droplet-string transition was investigated and found that the dispersed droplets could form a transient pearl necklace structure along the shear orientation [37–39]. Based on these great number of publications devoted to the structure formation in different emulsions or suspensions, the determined patterns in general depend on the rheological properties of a continuous medium as well as on the nature of dispersed particles or droplets. However, most tests in these studies were performed at relatively low temperatures. The dispersed phase is usually made of inorganic particles or low melting point liquid. In this paper, we report a shear-induced parallel cluster structure that formed from PA6 droplets covered with SEBS in a PP matrix at  $280 \text{ }^\circ\text{C}$ . Moreover, these parallel clusters were relatively stable and were aligned perpendicular to the direction of the shear flow. Our results are not only interesting from the viewpoint of fundamental polymer science but also may provide an approach to the formation of special structures and morphologies for industrial polymeric materials.

\*wjiang@ciac.jl.cn

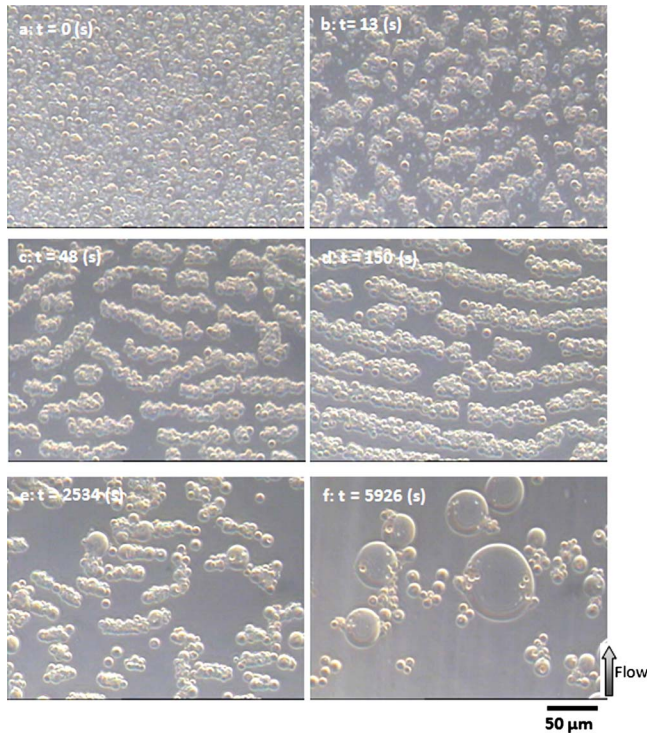


FIG. 1. (Color online) Evolution of morphologies from PA6-SEBS-PP blends at 280 °C. (a) Small PA6 droplets covered by SEBS (shear rate: 60  $s^{-1}$ ; shear time: 200 s). (b)–(d) Parallel cluster formation (shear rate: 2.5  $s^{-1}$ ). (e) and (f) Cluster rupture and coalescence into large spherical droplets (shear rate: 2.5  $s^{-1}$ ).

## II. EXPERIMENTAL METHOD

Polyamide 6 (PA6) and polypropylene (PP, 140) were supplied by Heilongjiang Nylon Plastic Factory (China) and Jilin Petrochemical Co., Ltd. (China), respectively. The average molecular weight ( $M_n$ ) and the polydispersity index ( $M_w/M_n$ ) of PP were  $7.74 \times 10^4$  and 5.47, respectively. The poly(styrene-ethylene-butadiene-styrene) (SEBS) (Kraton G1652;  $M_w$ : 45,000 g/mol; styrene content: 29 wt%) was obtained from Shell Development Co. The interfacial tension of the PA6 drops in the PP matrix is 7.2 mN/m at 230 °C. It reduces to 6.1 mN/m after adding 2 wt % SEBS into the PP matrix.

Shear tests were investigated online by employing a Linkam CSS 450 stage equipped with an Olympus BX-51 optical microscope. The sample was held in the gap between

the two quartz disks and was sheared by rotating the bottom disk using a precise motor, while the top disk remained stationary. In this manner, the microscopic structures existing during the shear process were visualized. The experiments were performed at  $280 \pm 1$  °C at a fixed gap width (40  $\mu\text{m}$ ). The masses of PA6, SEBS, and PP used were 2.9, 0.9, and 31.2 mg, respectively; i.e., their mass ratio was 8.3:2.6:89.1.

The rheological behavior at 280 °C was investigated using a Physica-200 rheometer and a 25 mm parallel plate.

## III. RESULTS AND DISCUSSION

Initially, we presheared the PA6-SEBS-PP mixture at a value of  $\dot{\gamma}$  of 60  $s^{-1}$  for 200 s and found that the small PA6 droplets partially covered by SEBS were randomly distributed in the PP matrix [Fig. 1(a)]. Similarly, Horiuchi *et al.* [40,41] reported that SEBS prefers to partly cover the interface between polycarbonate and polyamide 6. We set this as initial state and the time as zero. After decreasing the value of  $\dot{\gamma}$  abruptly to 2.5  $s^{-1}$ , we observed [Figs. 1(b)–1(d)] that the small droplets tended to aggregate and finally, at  $t = 150$  s, form a well-ordered pattern of parallel clusters. Migler *et al.* [37–39] found that the dispersed droplets from a polydimethylsiloxane-polyisobutylene mixture could form transient pearl necklace structures along the shear orientation. In our case, however, it is most interesting that these parallel clusters are not aligned along but are perpendicular to the direction of the shear flow. Moreover, the structure can be maintained more or less for a relatively long period of time (several tens of minutes) at  $\dot{\gamma} = 2.5$   $s^{-1}$ . This feature allowed us to freeze the structure by decreasing the temperature after cessation of the flow. For the purpose of clarity, we give a video showing the dynamic process of the formation of the parallel clusters in the supplementary material [42]. Based on Eq. (2), the average size of the PA6 droplets [Fig. 1(a)] should be equal to the stable steady-state droplet diameter ( $D_s$ ) at 60  $s^{-1}$ , and this size is much smaller than the  $D_s$  at 2.5  $s^{-1}$ . As a result, the PA6 droplets tend to coalesce into big ones once the shear rate decreases to 2.5  $s^{-1}$ . However, the SEBS cover at the PA6 droplets can retard the coalescence process. Therefore, the parallel cluster structure should be a metastable state. Eventually, these parallel clusters tended to aggregate into large, stable, spherical droplets [Figs. 1(e) and 1(f)] at the shear rate of 2.5  $s^{-1}$ .

Figure 2 presents schematic illustrations of the evolution of the morphologies formed from the PA6-SEBS-PP blends.

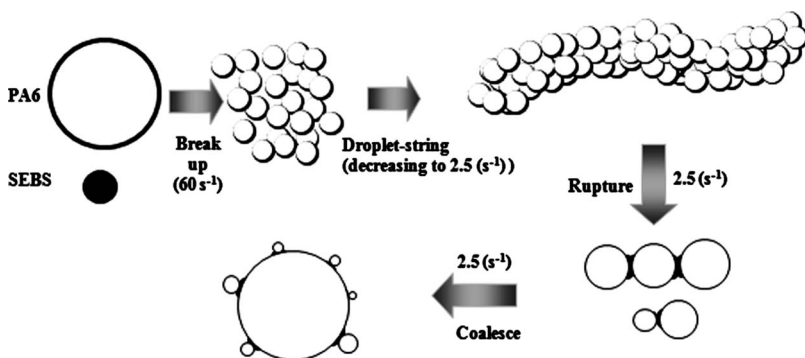


FIG. 2. Schematic illustration of the evolution of morphologies from PA6-SEBS-PP blends.

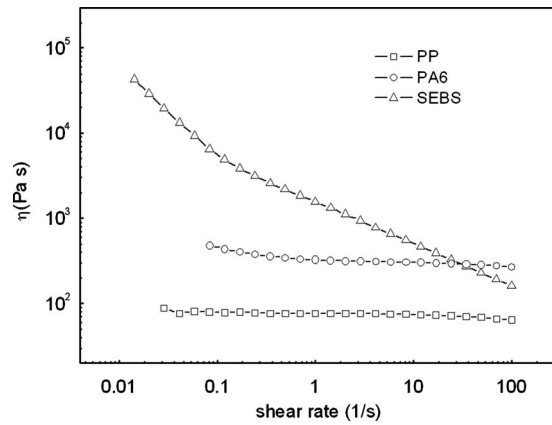


FIG. 3. Steady-shear viscosity plotted as a function of the shear rate for the pure melt components at 280 °C.

The process involves breakup, droplet-cluster transition, rupturing of clusters, and coalescence; SEBS behaves as a “glue” allowing neighboring PA6 droplets to form long parallel cluster structures and retarding their coalescence.

Figure 3 presents the shear viscosities at 280 °C for the pure melt components. The viscosity ratios were  $\lambda_1 = (\eta_0)_{SEBS}/(\eta_0)_{PP} = 81.5$  and  $\lambda_2 = (\eta_0)_{PA6}/(\eta_0)_{PP} = 6.1$ , where the terms  $(\eta_0)_{SEBS}$ ,  $(\eta_0)_{PA6}$ , and  $(\eta_0)_{PP}$  represent the viscosities of SEBS, PA6, and PP, respectively, at  $0.0838 \text{ s}^{-1}$ . Thus, the clusters that aggregated from the SEBS and PA6 droplets can be regarded as a highly viscous phase. The viscosity of the PP remained practically unchanged with respect to the shear rate. This result implies that the matrix phase can be considered approximately as a Newtonian fluid.

The phenomenon of individual droplets elongate perpendicular to the shear direction, i.e., vorticity elongation, has been observed before [23,24]. For instance, Hobbie and Migler [23] reported that the droplets in the polymeric emulsions extend in the shear direction at a low shear rate; however, these droplets become extended along the vorticity direction under a strong shear. They proposed that the transition behavior in the elongation direction is related to the change in first normal stress difference across the droplet interface. Moreover, Migler [24] also observed the shear-induced droplet vorticity alignment in the immiscible polymer blends. In the limit of weak shear and small droplets, the droplets tend to align along the shear direction, whereas for strong shear and large droplets, the droplet alignment is along the vorticity direction. From Refs. [24,25], it is clear that the droplets can slightly extend in the vorticity direction only when the emulsions are under a very strong shear. In the present study, however, PA6 droplets aggregate into long cluster structure with the glue effect of SEBS under a considerable low shear rate. Recently, Montesi *et al.* [25] reported the cylindrical flocs formed in the attractive emulsions and aligned along the vorticity direction also, which is very similar to present results. They also observed that these cylindrical flocs undergo a logarithmic rolling movement, which was, however, not observed in our experiments. In this work, we observed that the cylindrical clusters parallel shift in the flow. Montesi *et al.* [25] suggested that the clusters aggregating perpendicular to the flow direction is attributed

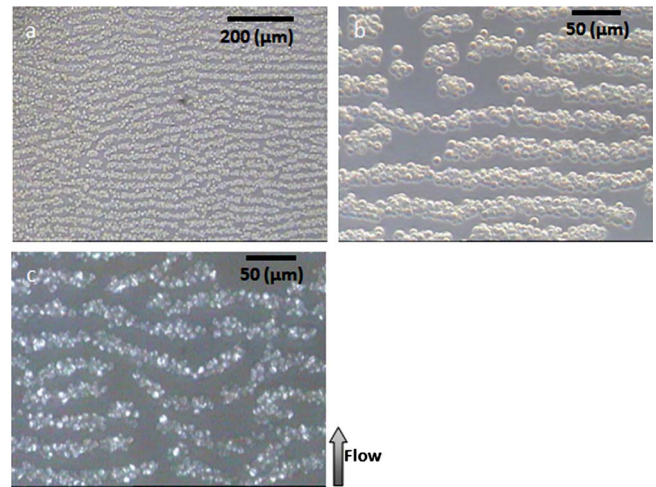


FIG. 4. (Color online) Optical micrographs and crossed polar micrographs of the clusters formed from PA6-SEBS-PP blends. (a) and (b) Optical micrographs of PA6-SEBS-PP blends (at  $2.5 \text{ s}^{-1}$  and 280 °C); 10 $\times$  and 40 $\times$  lenses, respectively. (c) Crossed polar micrograph of PA6-SEBS-PP blends at 175 °C after cessation of the flow.

to the existence of negative normal stresses ( $N1$ ). When  $N1$  is positive, the cluster is tensioned in flow direction and compressed in gradient direction, which will make the cluster elongate along the shear direction. However, the cluster can only extend to the vorticity direction if the cluster is subjected to compression in both flow and gradient directions, i.e.,  $N1$  is negative. Based on these points, it is proposed that the formation of the well-ordered cluster in present study is a result of cooperation of several factors. First, the glue effect of SEBS, comparable to the attractive force between the droplets in Montesi’s work [25], causes the formation of clusters. Second, the confinement effect imposed by the upper and lower disks in the experiment roughly determines the diameter ( $21 \mu\text{m}$ , comparable to the gap thickness of  $40 \mu\text{m}$ ) and ordering of the clusters. Moreover, the confinement effect also makes the sample compressed in the gradient direction, which prohibits the extension of cluster in gradient direction. Lastly, normal stresses arise from the high cluster elasticity, which causes the clusters extend perpendicular to the flow direction.

It is also worth noting that the patterns of parallel clusters [Figs. 4(a) and 4(b)] blend were reproducible at 280 °C. Af-

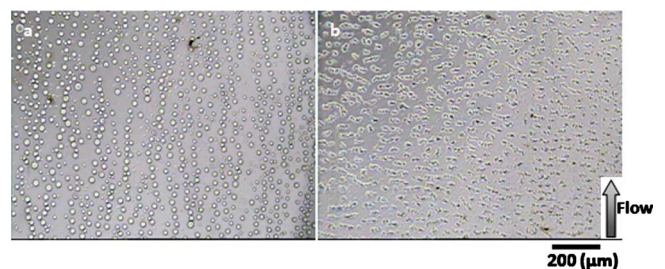


FIG. 5. (Color online) Optical micrographs of (a) PA6-PP and (b) SEBS-PP blends obtained under identical conditions, i.e., shearing for 200 s at  $60 \text{ s}^{-1}$  and 280 °C and then decreasing the shear rate abruptly to  $2.5 \text{ s}^{-1}$ .

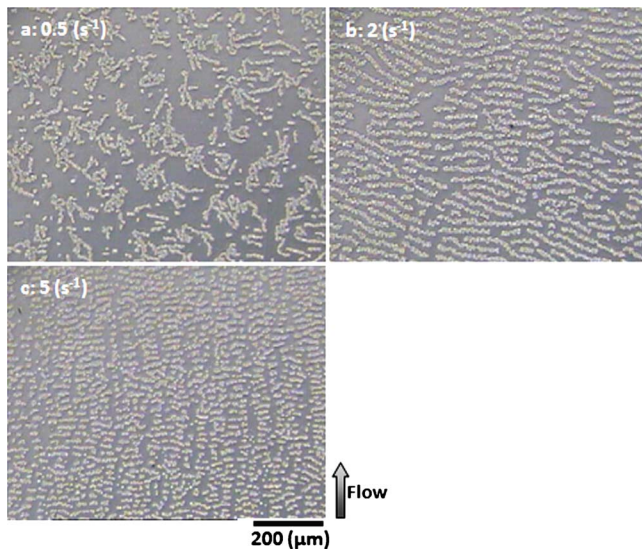


FIG. 6. (Color online) Optical micrographs of (a)–(c) PA6-SEBS-PP blends at various shear rates (temperature: 280 °C): (a)  $\dot{\gamma}=0.5 \text{ s}^{-1}$  (irregular clusters); (b)  $\dot{\gamma}=2 \text{ s}^{-1}$  (orderly long clusters); and (c)  $\dot{\gamma}=5 \text{ s}^{-1}$  (short rods).

ter cessation of the flow and then decreasing the temperature to 175 °C, at which PA6 can crystallize, led to the appearance of bright clusters in the PA6-SEBS-PP blends in the crossed polar micrograph [Fig. 4(c)]. Obviously, the bright regions observed at this temperature represent PA6 crystals. This finding suggests that the cluster pattern can be maintained by decreasing the temperature.

For the sake of comparison, we tested PA6-PP and SEBS-PP blends under the same conditions [Fig. 5]. For the PA6-PP blend, we found that the PA6 droplets were aligned along the direction of the shear flow in the PP matrix [Fig. 5(a)] at  $2.5 \text{ s}^{-1}$ . This result is similar to that observed for polyisobutylene-polydimethylsiloxane blends [37–39]. In contrast, the small SEBS droplets in the SEBS-PP blend were distributed uniformly in the PP matrix and a slight orientation of short SEBS droplets in the vorticity direction was also observed [Fig. 5(b)]. These results imply that the droplet-long scale cluster transition that we observed in this study occurred as a result of cooperation between PA6 and SEBS in the PP matrix at an appropriate shear rate.

In addition to the shearing time, the shear rate is another key factor that determines the formation of clusters. When we decreased the shear rate from  $60 \text{ s}^{-1}$  to a very low value of  $0.5 \text{ s}^{-1}$ , the droplets formed irregular clusters [Fig. 6(a)]; when we decreased the shear rate to a  $5 \text{ s}^{-1}$ , the droplets aggregated into very short rods and did not form cluster pattern either [Fig. 6(c)]. In contrast, when we decreased the shear rate to  $2 \text{ s}^{-1}$ , the well-defined cluster pattern reappeared [Fig. 6(b)]. Figure 7 presents the quantitative relationship between the average lengths of the aggregates droplets

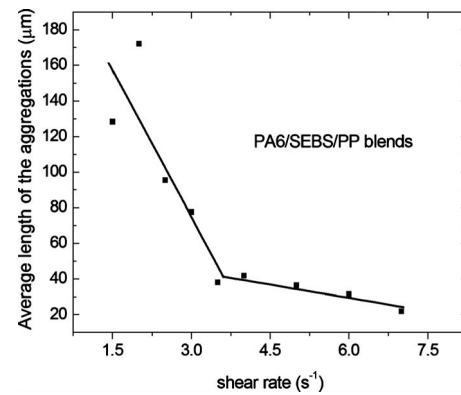


FIG. 7. Average length of the aggregates plotted as a function of the shear rate.

and the shear rate. The average lengths of the aggregates increased very slowly upon decreasing the shear rate to  $3.5 \text{ s}^{-1}$ . Thereafter, it increased markedly when decreasing the shear rate. The results indicate that a value of  $2 \text{ s}^{-1}$  is the most favorable shear rate for the formation of long clusters.

Our results imply that not only is shearing a main factor determining the sizes of the dispersed particles and their distribution but also it is a key factor that determines the arrangement of dispersed particles. Because shearing can induce the formation of unusual structures, it adds to the methods available for preparing well-ordered structures from polymeric systems [43,44]. We highlight the fact that all of the materials that we used in this study are commercial polymer products.

#### IV. CONCLUSIONS

We studied online the evolution of the morphologies and structures of PA6-SEBS-PP blends. Large drops of PA6 and SEBS formed randomly distributed small PA6 droplets covered by SEBS in the PP matrix under a high shear rate ( $60 \text{ s}^{-1}$ ). These droplets aggregated into well-ordered structures, i.e., parallel clusters, upon decreasing the shear rate abruptly to within the range of  $1.5\text{--}3.5 \text{ s}^{-1}$ . Interestingly, these parallel clusters were aligned perpendicular to the direction of the shear flow. An important feature of this system is that the well-ordered structures can be maintained for a long time (several tens of minutes) at the given shear rate; this feature allows us to freeze the structure by decreasing the temperature. Our results imply that control over the shear process allows polymer blends having well-ordered structures to be obtained.

#### ACKNOWLEDGMENTS

This work was financially supported by the National Natural Science Foundation of China (Grant Nos. 50725312, 50833005, 50930001, and 50921062). The authors would like to thank Professor Jan Mewis for useful discussions.

- [1] G. I. Taylor, *Proc. R. Soc. London, Ser. A* **138**, 41 (1932).
- [2] G. I. Taylor, *Proc. R. Soc. London, Ser. A* **146**, 501 (1934).
- [3] A. K. Chesters, *Chem. Eng. Res. Des.* **69**, 259 (1991).
- [4] J. M. H. Janssen, Ph.D. thesis, Eindhoven University of Technology, 1993.
- [5] J. M. H. Janssen and H. E. H. Meijer, *J. Rheol.* **37**, 597 (1993).
- [6] V. E. Ziegler and B. A. Wolf, *Macromolecules* **38**, 5826 (2005).
- [7] A. J. Ramic, S. D. Hudson, A. M. Jamieson, and I. Manas-Zloczower, *Polymer* **41**, 6263 (2000).
- [8] L. Levitt, C. W. Macosko, and S. D. Pearson, *Polym. Eng. Sci.* **36**, 1647 (1996).
- [9] R. Hayashi, M. Takahashi, H. Yamane, H. Jinnai, and H. Watanabe, *Polymer* **42**, 757 (2001).
- [10] K. S. Chang and W. L. Olbricht, *J. Fluid Mech.* **250**, 609 (1993).
- [11] C. Pozrikidis, *J. Fluid Mech.* **297**, 123 (1995).
- [12] S. Ramanujan and C. Pozrikidis, *J. Fluid Mech.* **361**, 117 (1998).
- [13] E. Lac, D. Barthes-Biesel, N. A. Pelekasis, and J. Tsamopoulos, *J. Fluid Mech.* **516**, 303 (2004).
- [14] E. Lac, A. Morel, and D. Barthes-Biesel, *J. Fluid Mech.* **573**, 149 (2007).
- [15] F. D. Rumscheidt and S. G. Mason, *J. Colloid Sci.* **17**, 260 (1962).
- [16] S. Torza, R. C. Cox, and S. G. Mason, *J. Colloid Interface Sci.* **38**, 395 (1972).
- [17] C. D. Han, *Multiphase Flow in Polymer Processing* (Academic, New York, 1981).
- [18] T. Hashimoto, K. Matsuzaka, E. Moses, and A. Onuki, *Phys. Rev. Lett.* **74**, 126 (1995).
- [19] S. Kim, E. K. Hobbie, J.-W. Yu, and C. C. Han, *Macromolecules* **30**, 8245 (1997).
- [20] A. Frischknecht, *Phys. Rev. E* **58**, 3495 (1998).
- [21] J. Delhomelle, J. Petracic, and D. J. Evans, *Phys. Rev. E* **68**, 031201 (2003).
- [22] W. G. P. Mietus, O. K. Matar, G. Seevaratnam, A. Wong, B. J. Briscoe, and C. J. Lawrence, *Phys. Rev. Lett.* **86**, 1211 (2001).
- [23] E. K. Hobbie and K. B. Migler, *Phys. Rev. Lett.* **82**, 5393 (1999).
- [24] K. B. Migler, *J. Rheol.* **44**, 277 (2000).
- [25] A. Montesi, A. A. Peña, and M. Pasquali, *Phys. Rev. Lett.* **92**, 058303 (2004).
- [26] J. Michele, R. Pgitzold, and R. Donis, *Rheol. Acta* **16**, 317 (1977).
- [27] L. Petit and B. Noetinger, *Rheol. Acta* **27**, 437 (1988).
- [28] M. A. Jefri and A. H. Zahed, *J. Rheol.* **33**, 691 (1989).
- [29] P. Poulin, H. Stark, T. C. Lubensky, and D. A. Weitz, *Science* **275**, 1770 (1997).
- [30] P. Poulin and D. A. Weitz, *Phys. Rev. E* **57**, 626 (1998).
- [31] M. K. Lyon, D. W. Mead, R. E. Elliott, and L. G. Leal, *J. Rheol.* **45**, 881 (2001).
- [32] I. I. Smalyukh, S. Chernyshuk, B. I. Lev, A. B. Nych, U. Ognysta, V. G. Nazarenko, and O. D. Lavrentovich, *Phys. Rev. Lett.* **93**, 117801 (2004).
- [33] B. J. Luther, G. H. Spring, and D. A. Higgins, *Chem. Mater.* **13**, 2281 (2001).
- [34] V. G. Nazarenko, A. B. Nych, and B. I. Lev, *Phys. Rev. Lett.* **87**, 075504 (2001).
- [35] M. Yada, J. Fukuda, J. Yamamoto, and H. Yokoyama, *Rheol. Acta* **42**, 578 (2003).
- [36] S. Lin-Gibson, J. A. Pathak, E. A. Grulke, H. Wang, and E. K. Hobbie, *Phys. Rev. Lett.* **92**, 048302 (2004).
- [37] K. B. Migler, *Phys. Rev. Lett.* **86**, 1023 (2001).
- [38] J. A. Pathak, M. C. Davis, S. D. Hudson, and K. B. Migler, *J. Colloid Interface Sci.* **255**, 391 (2002).
- [39] J. A. Pathak and K. B. Migler, *Langmuir* **19**, 8667 (2003).
- [40] S. Horiuchi, N. Matchariyakul, K. Yase, and T. Kitano, *Macromolecules* **30**, 3664 (1997).
- [41] C. H. Lee, Y. M. Lee, H. K. Choi, S. Horiuchi, and T. Kitano, *Polymer* **40**, 6321 (1999).
- [42] See supplementary material at <http://link.aps.org/supplemental/10.1103/PhysRevE.82.031807> for a video showing the dynamic process of the assembly of parallel clusters from disordered droplets.
- [43] Y. H. Na, T. Shibuya, S. Ujiie, T. Nagaya, and H. Orihara, *Phys. Rev. E* **77**, 041405 (2008).
- [44] D. R. E. Snoswell, A. Kontogeorgos, J. J. Baumberg, T. D. Lord, M. R. Mackley, P. Spahn, and G. P. Hellmann, *Phys. Rev. E* **81**, 020401 (2010).